



# The distance from the Sun to the centre and the shape of the old bulge in the Galaxy: 16 221 OGLE RR Lyrae stars

Evgeny Griv,<sup>1</sup> Michael Gedalin,<sup>1</sup> Paweł Pietrukowicz,<sup>2</sup> Daniel Majaess<sup>3</sup> and Ing-Guey Jiang<sup>4</sup>

<sup>1</sup>Department of Physics, Ben-Gurion University of the Negev, Beer-Sheva 8410501, Israel

<sup>2</sup>Astronomical Observatory, University of Warsaw, Al. Ujazdowskie 4, PL-00-478 Warszawa, Poland

<sup>3</sup>Department of Astronomy and Physics, Saint Mary's University, Halifax, Nova Scotia B3H 3C 3, Canada

<sup>4</sup>Department of Physics and Institute of Astronomy, National Tsing-Hua University, Hsin-Chu 30013, Taiwan

Accepted 2020 September 7. Received 2020 August 31; in original form 2020 May 1

## ABSTRACT

A statistical method is used to determine both the Sun's distance  $r_0$  from the Galactic Centre and the 3D structure of the old stellar population of the Galactic bulge. The space distribution of 16 221 high latitude type-RRab RR Lyrae stars from the optical OGLE survey located towards the bulge is explored. An estimate by using RR Lyraes leads to a mean  $r_0 = 8.28 \pm 0.14$  kpc within the effective bulge radius of  $r_{\text{bulge}} = 2\text{--}3$  kpc. The distribution of RR Lyraes within  $r_{\text{bulge}}$  has the shape of an ellipsoid slightly elongated almost towards the Sun with a major axis of its symmetry  $a$  and two minor axes  $b$  and  $c$  of about the same length. The axial ratio is  $a: b: c \approx 1: 0.7: 0.7$ . These age-old, metal-poor, and kinematically hot stars do not trace a strong bar-like structure in the direction of the bulge at distances  $> 1$  kpc from the Galactic Centre, as  $b/a \sim 1$ .

**Key words:** Galaxy: bulge – Galaxy: fundamental parameters – Galaxy: kinematics and dynamics – Galaxy: structure.

## 1 INTRODUCTION

Several fundamental constants are used to describe the Milky Way Galaxy, an Sb–Sbc-type barred spiral galaxy. Among them are the radial distance from the Sun to the Galactic Centre (GC), the scale length ratio of the major axis to the minor axis in the plane and to the vertical axis of both a halo and a bulge space distributions, and the length and orientation of the bar-shaped central regions.

### 1.1 Solar distance

In any dynamical model of the Galaxy, the Galactocentric distance of the Sun,  $r_0$ , plays a fundamental role (Reid 1993; Genzel, Eisenhauer & Gillessen 2010; Bland-Hawthorn & Gerhard 2016). In particular, its value has great impact on distance and mass estimates of objects throughout the system under study. Its value is also crucial for developing the rotation curve of the system, which may help us to understand the overall mass distribution and may be able to provide insight to the dark matter mass contribution. Actually, the problem of deriving  $r_0$  has not been unambiguously resolved and it is worthwhile to determine its value by using new observational data and better mathematical methods.

The solar distance  $r_0$  has recently been estimated by the *direct* method (see Genzel et al. 2010 for an explanation) from the distances to various astronomical objects. Using the VLBA of the National Radio Astronomy Observatory and the Japanese VERA project, Reid et al. (2019) have analysed  $\approx 200$  trigonometric parallaxes and proper motions of molecular masers associated with very young ( $< 10^5$  yr) massive stars. Modelling the 3D space motions has yield the estimate

of  $r_0 = 8.15 \pm 0.15$  kpc. Measurements of the radial velocity and proper motion for the GC S2 star orbiting the massive  $\approx 4 \times 10^6$   $M_\odot$  black hole Sgr A\* (Genzel et al. 2010) in the framework of the general theory of relativity yield a marginally lower value of

$$r_0 = 7946 \pm 50 \text{ (statistical error)} \pm 32 \text{ (systematic error)} \text{ pc}$$

(Do et al. 2019).<sup>1</sup> GRAVITY Collaboration (2019) also monitored the radial velocity and motion on the sky of S2 star for 27 yr, with the SINFONI and NACO adaptive optics instruments on the ESO's VLT, and added near-infrared interferometry with the VLTI beam combiner. An unprecedented accurate geometric distance evaluation of

$$r_0 = 8178 \pm 13 \text{ (stat)} \pm 22 \text{ (sys)} \text{ pc}$$

was obtained. Notice that Do et al. (2019) and GRAVITY Collaboration (2019) exploited the exact same object, although with different data sets. Besides the data set, the two groups also differ in the astrometric reference system they employ. de Grijs & Bono (2016) have compiled the most comprehensive and most complete data base of GC distances available to the end of 2015. They obtained a statistical determination of  $r_0 = 8.3 \pm 0.2 \text{ (stat)} \pm 0.4 \text{ (sys)} \text{ kpc}$ . See also Boehle et al. (2016), Fritz et al. (2016), Bhardwaj et al. (2017), McMillan (2017), Contreras Ramos et al. (2018), Majaess et al. (2018), and Qin et al. (2018) for the latest since 2016 less accurate measurements of  $r_0$  in the wide range 7.9–8.5 kpc by

<sup>1</sup>Do et al. (2019) exploited a total of 45 astrometric positional measurements spanning 24 yr at the W. M. Keck Observatory and 115 radial velocity measurements (18 yr) at the W. M. Keck Observatory, Gemini North Telescope, and Subaru Telescope to fit the 16-yr orbit of S2 around the Sgr A\*.

\* E-mail: griv@bgu.ac.il

applying both direct and indirect approaches. A compilation of 28 independent measurements by Camarillo et al. (2018) has provided the probably most respectable estimate of  $r_0 = 8.0 \pm 0.3$  kpc ( $2\sigma$  error). Thus, in recent years, the 1985 IAU recommended value of  $r_0 = 8.5$  kpc (Kerr & Lynden-Bell 1986) has been challenged, claiming a somewhat smaller value.

Specifically, given the precision of the direct methods, they are preferable over the indirect ones (Genzel et al. 2010, p. 3160). Nevertheless, in view of the  $\sim 3\sigma$  disagreement between the Do et al. (2019) and GRAVITY Collaboration (2019) solar distances and the possibility of employing large-scale APOGEE-2, *Gaia*-ESO, GALAH, 4MOST, and LAMOST sky surveys for thousands and even millions of stars (e.g. Queiroz et al. 2020), we intend to use a variety of observational data to determine the basic parameters of the Galaxy by using the *indirect* statistical method, and to demonstrate the effectiveness of the approach. Interestingly, in the reverse case the firm distance of the GC can help us determine, for example, the RR Lyrae stars (RRLs) distance scale and the effect of extinction on it.

## 1.2 Shape of the old bulge

The Galactic bulge with a stellar mass of  $\approx 2 \times 10^{10} M_\odot$  contains about 10–20 per cent of the visible mass of the system (Valenti et al. 2016; Simion et al. 2017). There is a key model discussed in the literature for the radial distribution of matter in the spherical-like, almost non-rotating, primarily pressure-supported old bulge (and halo) subsystems. We can characterize the 3D distribution of stellar populations in the Galactocentric Cartesian coordinate system: the  $Y$ -axis points to the direction of the Galactic rotation, the  $X$ -axis points to the Galactic anticentre, the  $Z$ -axis points to the North Galactic pole. We observe an ellipsoid of  $N$  objects with normalized axes  $a$  (and  $a \equiv 1$ ) directed to us and  $b$  in the  $X$ - $Y$  plane and an axis  $c$  perpendicular to this plane. Ellipsoidal isodensity contours for the subsystem can be expressed as

$$\frac{x^2}{a^2} + \frac{y^2}{b^2} + \frac{z^2}{c^2} = 1, \quad (1)$$

where  $(x, y, z)$  are the Cartesian coordinates centred on the GC. The spherical model ( $a = b = c$ ) is the most basic. The case of a spheroidal subsystem has  $b = c$  and flattening described by  $q = c/a$ . In the case of a triaxial ellipsoidal subsystem  $a \neq b \neq c$ .

The oblateness of the Galactic globular cluster halo is  $q \approx 0.8$  (Harris 1976; Freeman & Norris 1981; Zinn 1985; Bonatto et al. 2009). The oblateness of the stellar halo is also  $q = 0.7$ –0.9 (Sesar, Jurić & Ivezić 2011). Pietrukowicz et al. (2015) considered a sample of about 4700 RRLs in a small rectangular region defined in Galactic coordinates as  $-4^\circ < l < +4^\circ$ ,  $-6.9^\circ < b < -2.7^\circ$  from the whole available sample of the 27 258 objects of the latest Optical Gravitational Lensing Experiment (OGLE) survey in the old bulge. The scale length ratio of the major axis of the symmetry to the minor axis in the plane and to the vertical axis of an ellipsoid within  $\approx 1$  kpc from the GC was found to be  $a: b: c \approx 1: 0.5: 0.4$ . The VVV survey data demonstrate an ellipsoidal distribution of red clump stars (or relatively metal-rich red horizontal branch stars) within the central 4 kpc bulge with an axial ratio of  $\approx 1: 0.44: 0.31$  (Simion et al. 2017). The *Gaia* DR2 set of intermediate-age long-period Mira variables throughout the Galaxy disc and bulge also shows that the bulge is well modelled by a triaxial ellipsoidal distribution with an axial ratio of  $\approx 1: 0.4: 0.3$  and with an effective bulge radius of  $r_{\text{bulge}}$  in the range 2–3 kpc (Majaess, Turner & Lane 2009, p. 266; Grady, Belokurov & Evans 2020).

In the Galaxy, the radial distribution of matter in the bulge (and halo) therefore is roughly circularly symmetric. Radial velocities of round 1000 RRLs located towards the bulge indicate that these stars form a spheroidal, pressure-supported component (Kunder et al. 2016). Prudil et al. (2019) did not observe any spatial correlation with the non-axial symmetric bar for both Oosterhoff groups of 8141 fundamental-mode RRLs. Over 30 yr ago, Wesselink (1987) has already studied the RRLs in low-latitude regions towards the bulge, not finding a connection to the bar. In relation to this, Alcock et al. (1998) have noted that only the RRLs in the inner regions closer to the GC show a barred distribution, presumably where the bar potential is strong enough to influence the kinematically hot RRLs component. In the spirit of Harris (1976), Freeman & Norris (1981), Zinn (1985), Miceli et al. (2008), Mateu & Vivas (2018), and many others (e.g. Sesar et al. 2011), the spatial density of objects can be described by the ordinary power-law  $\rho(r) \propto r^\alpha$ , where  $r$  is the Galactocentric distance and the power-law index  $\alpha$  is negative. Such a simple power-law model can be applied to bulge's objects located at distances  $0.2 \lesssim r \lesssim 4$  kpc from the GC (Pietrukowicz et al. 2015, fig. 4 therein; Saha et al. 2019, fig. 22 therein). There is a rise in the RRLs density beyond  $r \sim 5$  kpc (Saha et al. 2019, fig. 23 therein).

## 1.3 Parameters of the bar

Oval-like distortions or bars are a very common feature of disc galaxies. Only less than about 25 per cent of spiral galaxies can be classified as non-barred galaxies (Elmegreen & Elmegreen 1989; Aguerri, Méndez-Abreu & Corsini 2009). Strong and weak bars have been found in the vast majority of disc galaxies in the local Universe (Buta et al. 2015). As regards our own Galaxy, the presence of the bar spaced in the central regions of the system which likely formed  $\approx 8$ –9 Gyr ago has been unambiguously established in the 1990s (Weiland et al. 1994; Binney, Gerhard & Spergel 1996; López-Corredoira et al. 1997; see also Anders et al. 2019; Bovy et al. 2019; Clarke et al. 2019; Grady et al. 2020). Both planar gas and intermediate-age stars, for example, red clump stars that are predominantly metal rich, trace a strong bar at all latitudes (e.g. Kunder & Chaboyer 2008; Majaess 2010). It is important to note that the spatial distribution of the old metal-poor RRLs *differs* from the structures traced by the metal-rich stars. The metal-poor stars do not trace a strong bar, but have a more spheroidal, centrally concentrated distribution, showing only a slight elongation in its innermost  $\lesssim 1$  kpc parts (Dékány et al. 2013; Minniti et al. 2017; Prudil et al. 2019). Catchpole et al. (2016) and Grady et al. (2020) have also argued that the longer period Mira variables (age  $\sim 5$  Gyr and younger), which trace an intermediate-age population, give evidence of a bar inclined to the line of sight in the bulge. But the shorter period Miras with ages  $\sim 9$  Gyr and older do not show this.

At present, the bar size and orientation parameters are still being disputed. The majority of experts in the field support a model of a short, rapidly (and rigidly) rotating bar with a semimajor axis of no more than  $r_{\text{bar}} = 3$  kpc (Binney et al. 1996; Antoja et al. 2014; Sormani, Binney & Magorrian 2015; Bovy et al. 2019; Grady et al. 2020; Hinkel, Gardner & Yanny 2020). Other authors discuss a model of a long-slow bar with  $r_{\text{bar}} = 4$ –5 kpc (Wegg, Gerhard & Portail 2015; Portail et al. 2017; see also Sanders, Smith & Evans 2019). The axial ratio is  $\approx 1: 0.4: 0.3$  (Rattenbury et al. 2007). See Bland-Hawthorn & Gerhard (2016) for a discussion. The general consensus is that the underlying non-axisymmetric features of the Galaxy – logarithmic spiral arms and bar – rotate at different pattern speeds and the bar rotates faster than the spiral arms (Griv et al. 2020; Khoperskov et al. 2020; Pettitt, Ragan & Smith 2020).

In the inner regions of the Galaxy, the barred structure of RRLs, intermediate-age red clump, and red giant branch stars inclined at an angle of  $\theta = 20^\circ\text{--}30^\circ$  with respect to the line of sight between the Sun and the GC, with the near end in the first Galactic longitude quadrant (Babusiaux & Gilmore 2005; Bobylev et al. 2014; Pietrukowicz et al. 2015; Wegg et al. 2015; Simion et al. 2017).

#### 1.4 Objectives of the paper

In our previous publication (Griv, Gedalin & Jiang 2019), we have reported the indirect estimation of  $r_0$  from the space distribution of objects of the spherical halo in the Galaxy at distances of up to  $\sim 25$  kpc from the GC by using the maximum likelihood statistical method. The method was originally proposed by Rastorguev et al. (1994) and subsequently modified in our work. It was suggested that the centre of the entire old Galactic population coincides with the GC. The investigation was restricted to observational data up to 2008. The Harris (1996) catalogue of  $\approx 160$  globular clusters and the SEKBO survey catalogue of  $\approx 2000$  RRLs of Keller et al. (2008) situated in the halo were explored. We have found that the RRLs are more convenient objects for our aim. This is because the distances are reasonably accurate for RRLs – more so than for coeval globular clusters. We have also found that as no data are available of the stars in the inner regions of the halo at distances  $r < 5\text{--}8$  kpc from the GC, currently the more extensive Drake et al. (2013) and Sesar et al. (2013, 2017) samples of RRLs cannot be used to calculate  $r_0$  by using the method.

In this connection, measurements of great importance of distances from the Sun have recently been done for RRLs in the Galaxy. Pietrukowicz et al. (2015) and Soszyński et al. (2019) have detected thousands of fundamental-mode RRLs toward the Galactic bulge from data collected during the fourth phase of the OGLE.<sup>2</sup> Let us exploit these new observational data to determine the solar distance and shape of the old bulge population in the system.

Our objectives with this study are twofold. First, we correct our value for  $r_0$  provided by latest observational data up to the end of 2019. Second, unlike Griv et al. (2019), we determine the shape of the spatial distribution of power-law bulge objects, in particular, the axial ratio of an observed ellipsoid of stars and the inclination angle  $\theta$ . The important question about the geometry of the possible bar is also addressed. To emphasize it again, our computational method will be applied to the latest OGLE sample of RRLs with known photometric distances; these will yield the foregoing solar distance and shape of the bulge.

Majaess et al. (2018) have also identified 4189 type-RRab RRLs in the old Galactic bulge with the near-infrared VVV survey photometry for high latitude stars.<sup>3</sup> Both stellar samples, from VVV and OGLE,

cover almost the same bulge area, but the distances to the stars are calculated in a different way. Generally, infrared VVV data have some advantages over optical OGLE studies. In particular, an increase in the precision of both the absolute magnitudes and individual reddening values and more accurate the VVV  $K_s$ -band average magnitudes than the OGLE  $V$ -band ones yield more precise distances (Dékány et al. 2013; Majaess et al. 2018). On the other hand, the two sets have significantly different sizes and partly overlap. We have cross-matched the VVV and OGLE samples. It turns out that 2408 stars are in common, thus strengthening the candidate classifications of two research pushes. This is about 15 per cent of the whole OGLE sample. In addition, 483 VVV detections do not have OGLE counterparts. We have gone through a random 10 light curves and found that the objects are eclipsing binaries, not RRLs at all. The OGLE set is about 4 times larger than the VVV one, highly complete (at higher latitudes), and very pure. In this study, in order to investigate the 3D structure of the bulge population we take only the OGLE set with distances measured from the optical bands.

This paper is organized as follows. In Section 2, selection of the observational data and formation of volume-limited sets are described. The method explored in the study is detailed in Section 3. Modelling process and results of model calculations are presented in Section 4. Discussion of the main results and the summary follow in Section 5.

## 2 OBSERVATIONAL MATERIAL

RRLs with ages  $\gtrsim 10$  Gyr are well-known tracers of age-old stellar populations. Generally, RRLs are distributed from the innermost regions to the outer halo of the Galaxy. The bulk rotation of this metal-poor population is negligible. The population is mainly supported dynamically by random velocity dispersion and probe the structure of the ancient, spherical-like, almost non-rotating component from the inner bulge to the periphery of the system (Drake et al. 2013; Kunder et al. 2016; Sesar et al. 2017; Contreras Ramos et al. 2018). In the Galaxy, RRLs represent  $\sim 1$  per cent of the bulge population (Pietrukowicz et al. 2012; Nataf et al. 2013).

The original OGLE sample from Soszyński et al. (2014) contains 27 237 objects. The selection of objects was conducted in three steps. After rejection of globular cluster members, foreground (Galactic disc) and background (Sgr dSph) objects, leaving only variables with both  $I$ - and  $V$ -band measurements, we obtained a set of 21 026 RRLs. The  $V$ -band information was needed in the distance determination. To explore the structure of the old bulge population, we have to work on a complete set of only bulge stars and to assume that in selected directions we see all of them. Of course, regions close to the plane are highly incomplete in the optical regime. For the purpose of our analysis, we prepared a map of such ‘complete’ directions (Pietrukowicz et al. 2015). In our calculations, we used the near-IR reddening map from Gonzalez et al. (2012) which covers a rectangle narrower than the OGLE coverage. These steps shrinked the sample of stars with determined distance to 16 221 type-RRab RRLs. Pietrukowicz et al. (2015) have obtained the Galactic longitudes  $l$ , latitudes  $b$  (not to be confused with the minor axis  $b$  of the observed ellipsoid of stars), and the line-of-sight (heliocentric) distances  $d$  of each of these stars.

Especially notice that Pietrukowicz et al.’s (2015) heliocentric distances are adopted along with their possible biases. The bulge

<sup>2</sup>The OGLE project is a sky survey conducted since the early 1990s by astronomers associated with the University of Warsaw Astronomical Observatory. Observations are carried out with the 1.3 m fully automated, computer controlled, Ritchey–Chretien system Warsaw Telescope at the Las Campanas Observatory. Main goals are the detection and classification of pulsating and eclipsing variable stars, discoveries of the microlensing events, dwarf novae, and investigations of the Galaxy structure and the Magellanic Clouds (Udalski, Szymański & Szymański 2015; Pietrukowicz 2020).

<sup>3</sup>By using the 4.1 m wide-field reflecting VISTA telescope for the Southern hemisphere in Chile for a 5 yr period, the VISTA Variables in the Via Láctea (VVV) ESO Public Survey aims to probe the 3D structure of the Galactic bulge and adjacent regions of the disc utilizing various distance indicators (Minniti et al. 2010; Saito et al. 2012; Minniti et al. 2017; Surrot et al. 2019). Deep near-infrared observations are performed towards the bulge in

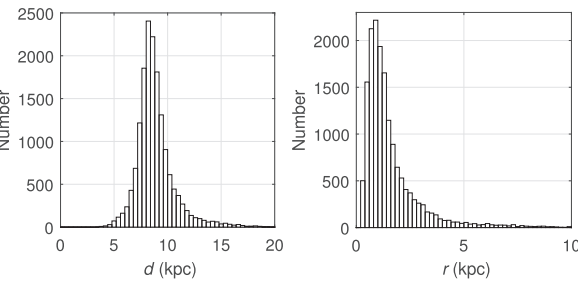


**Figure 1.** Distributions of all selected 16 221 RRLs from the OGLE sample with respect to  $d$  and  $r$ , assuming  $r_0 = 8.1$  kpc.

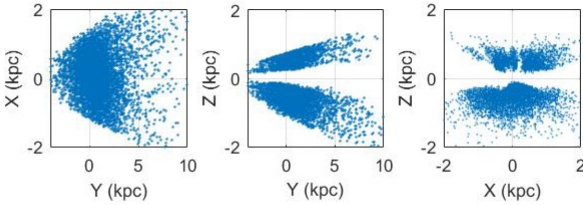


**Figure 2.** Spatial distribution of RRLs in a special Cartesian ( $X$ ,  $Y$ ,  $Z$ ) coordinate system centred on the GC, with the Sun at  $(0, 8.1, 0.02)$ .

VVV photometry had inherent photometric biases due to the zero-point calibration method adopted for the survey, which has been claimed to have directly propagated both into the extinction law study of Nataf et al. (2013), as well as into the colour excess maps of Gonzalez et al. (2012), propagating further into the RRLs distance estimates of Pietrukowicz et al. (2015). Hajdu et al. (2020) have identified two independent sources of bias in the photometric zero-points of the standard calibration procedure of VVV data in the  $J$ ,  $H$ , and  $K_s$  passbands. Recommendations have been given for future improvements of the pipeline calibration of VVV photometry.

The Galactocentric distance  $r$  of a star can be derived from the equation

$$\begin{aligned} r^2 &= (r_0 - d \cos b \cos l)^2 + d^2 \cos^2 b \sin^2 l \\ &\quad + (d \sin b + z_0)^2, \end{aligned} \quad (2)$$

where  $z_0$  is the Sun's distance from the mid-plane. We assume that the Sun lies slightly  $z_0 = 20$  pc above the equatorial  $z = 0$  plane. The error of  $z_0$  is of the order of just a few parsecs (Majaess et al. 2009; Ferguson, Gardner & Yanny 2017; Bennett & Bovy 2019; Skowron et al. 2019). The centre of the Galaxy, as marked by Sgr A\*, in Galactic coordinates is slightly offset from  $l = 0^\circ$  and  $b = 0^\circ$ , but this does not affect the conclusions at the precision offered by RRLs (e.g. Gillessen et al. 2009; Genzel et al. 2010).

Fig. 1 compares the heliocentric and Galactocentric distributions of all selected 16 221 OGLE RRLs. As is seen, for regions of  $r > 1$  kpc the stars show a centrally concentrated distribution and the spatial density of stars can indeed be described by a power law. In the calculation, we restricted ourselves to objects within the regions of  $r = r_{\max} < 3 - 4$  kpc (for  $r_0 = 8.1$  kpc). Less than 10 per cent of all RRLs are localized beyond the limit  $r_{\max}$  in the range 3–4 kpc, and thus the contribution of these distant objects to the likelihood function (see Section 3 for the definition) is expected to be rather small.

Space locations of RRLs in a Cartesian  $XYZ$  frame are shown in Fig. 2. The sky distribution of objects is not uniform. The expected concentrations to the GC and the mid-plane are clearly seen.

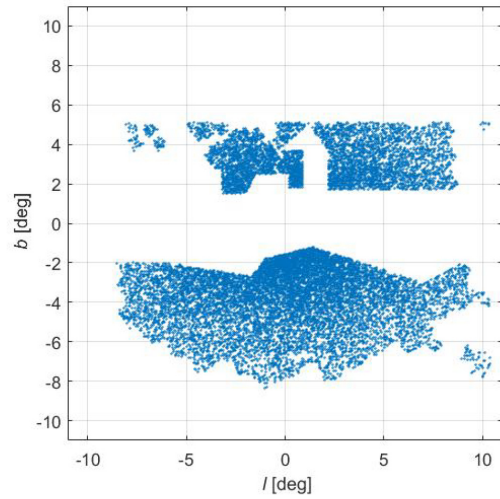


**Figure 3.** Galactic coordinates of the sample of RRLs in the bulge area.

For easier visibility of the sample, Fig. 3 displays the location of RRLs in the Galactic coordinates  $l$  and  $b$ . Stars of the sample cover almost all bulge area, excluding the  $|b| \lesssim 2^\circ$  belt. At  $|b| \lesssim 2^\circ$ , extinction by interstellar dust concentrated along the Galactic plane draws the apparent magnitudes of RRLs beyond the faint detection limit of the OGLE survey. Thus, the sample does not cover regions close to the GC and the Galactic equatorial plane (cf. Fig. 2). This is important for our study, because closer to the GC and the equatorial plane, extinction because of strong dust obscuration towards the inner Galaxy proportional to  $(1 - \text{const} \times \cos l)$  and  $\exp[-\text{const}/(|\sin b| + \text{const})]$ , respectively, causes the completeness of the sample to drop essentially (Rastorguev et al. 1994; see also Gonzalez et al. 2012, fig. 3 therein; Dékány et al. 2013, fig. 2 therein). This is why the high latitude OGLE sample of stars which was specifically done for high latitude ( $|b| \gtrsim 2^\circ$ ) objects attracts our attention.

Pietrukowicz et al. (2015) give no individual statistical errors of the distance of a star from the Sun. We accept for individual errors of  $d$  an average value equal to  $\pm 5$  per cent. The rather accurate stellar distances and substantial number of objects in the sample should assure truthful results.

### 3 METHOD OF CALCULATION

The standard equation for the ellipse in the  $XYZ$  coordinate system is given by equation (1). Next, following closely Pietrukowicz et al. (2015), we rotate the  $XYZ$  system through the clockwise angle  $\theta$ . The equation for the ellipse in this new coordinate system is obviously

$$\frac{(x \cos \theta + y \sin \theta)^2}{a^2} + \frac{(x \sin \theta - y \cos \theta)^2}{b^2} + \frac{z^2}{c^2} = 1, \quad (3)$$

where  $(x, y, z)$  are the Galactocentric Cartesian coordinates of objects and  $\theta$  is the tilt angle, which defines the orientation of the major axis of the ellipsoid. The radial distribution of matter in the non-rotating subsystem is nearly spherical and the spatial density of objects is described by the power law

$$\rho(r) = \text{const} \times (r/\text{const})^\alpha, \quad (4)$$

where  $\alpha < 0$ .

We turn now to the procedure for determining the quantities  $r_0$ ,  $\alpha$ ,  $\theta$ ,  $a$ ,  $b$ , and  $c$  from observations. The observed space distribution

**Table 1.** Data on the number of selected objects  $N$ , solar distance  $r_0$ , power-law index  $\alpha$ , tilt angle  $\theta$ , normalized major axis of the symmetry of the ellipsoid  $a$  and the minor axis  $b$  in the plane, and vertical axis  $c$  within the adopted distance  $r_{\max}$  from the GC, obtained with the OGLE sample of 16 221 RRLs.

$r_{\max}$ (kpc)	$N$	$r_0$ (kpc)	$\alpha$	$\theta$ (deg)	$a$	$b$	$c$
1.5	10 584	$8.12 \pm 0.17$	$-1.58 \pm 0.04$	$+1.5 \pm 0.5$	1.0	$0.96 \pm 0.03$	$0.93 \pm 0.04$
2.0	12 672	$8.23 \pm 0.15$	$-2.12 \pm 0.05$	$-3.0 \pm 0.7$	1.0	$0.88 \pm 0.04$	$0.81 \pm 0.03$
2.5	13 811	$8.23 \pm 0.14$	$-2.36 \pm 0.04$	$-11.5 \pm 0.8$	1.0	$0.71 \pm 0.03$	$0.67 \pm 0.03$
3.0	14 539	$8.37 \pm 0.14$	$-2.45 \pm 0.05$	$-5.0 \pm 0.3$	1.0	$0.62 \pm 0.04$	$0.61 \pm 0.03$
3.5	15 035	$8.37 \pm 0.16$	$-2.60 \pm 0.03$	$-5.5 \pm 0.4$	1.0	$0.56 \pm 0.02$	$0.55 \pm 0.02$
4.0	15 334	$8.27 \pm 0.15$	$-2.70 \pm 0.04$	$-3.0 \pm 0.2$	1.0	$0.53 \pm 0.03$	$0.53 \pm 0.03$

function of objects is represented by the following expression:

$$f(x, y, z) = \mathcal{A}(r_0, \dots, c)(r/\text{const})^\alpha \quad (5)$$

with the normalization condition

$$\int_V f(x, y, z) dx dy dz = 1, \quad (6)$$

where  $(x, y, z)$  are the rederived coordinates of objects,  $\mathcal{A}$  is the unknown normalization factor,  $(r_0, \dots, c)$  are the parameters of the spherical-like distribution function  $f(x, y, z)$  (Rastorguev et al. 1994). In the general case of ellipsoidal distribution of objects within the region  $r_{\min} \leq r \leq r_{\max}$ , we rewrite the normalization condition given by equation (6) as

$$4\pi abc \mathcal{A} \int_{r_{\min}}^{r_{\max}} \tilde{r}^2 (\tilde{r}/r_{\max})^\alpha d\tilde{r} = 1, \quad (7)$$

where  $a = x_{\max}/r_{\max}$ ,  $b = y_{\max}/r_{\max}$ ,  $c = z_{\max}/r_{\max}$ ,  $x = aX$ ,  $y = bY$ ,  $z = cZ$ , and  $\tilde{r}^2 = X^2 + Y^2 + Z^2$ . Thus,

$$\mathcal{A} = \frac{\alpha + 3}{4\pi abcr_{\max}^3} \frac{1}{1 - \beta^{\alpha+3}}, \quad (8)$$

where  $\beta = r_{\min}/r_{\max}$ .

Let us now define the standard likelihood function as a joint probability distribution. Because the data points  $r_1, \dots, r_N$  for a given  $r_0$  are independent of each other, the joint probability distribution is the product of the individual distributions. The likelihood function is then

$$L(r_0, \dots, c) = \prod_{i=1}^N f(r_i; r_0, \dots, c). \quad (9)$$

One has to recalculate the Galactocentric distances of individual objects  $r_i$  and the normalization factor  $\mathcal{A}$  according to equations (2), (3), and (8) at each reference to the basic equation (9). We find the six parameter values  $r_0, \alpha, \theta, a, b$ , and  $c$  that maximize  $L$ . The expression (9) depends on  $(r_0, \dots, c)$  in a non-linear fashion, so it is a problem how to derive their error estimates for such a non-linear fit. This can be addressed using a numerical modelling approach (Pavlovskaya & Suchkov 1980; Griv et al. 2014).

## 4 RESULTS OF CALCULATION

In the calculation, maximization of  $L$  was done in the six-dimensional parameter space for stars. For each values of parameters from initial  $r_{0,\min}, \alpha_{\min}, \theta_{\min}, a_{\min}, b_{\min}$ , and  $c_{\min}$  to final  $r_{0,\max}, \alpha_{\max}, \theta_{\max}, a_{\max}, b_{\max}$ , and  $c_{\max}$ , we have solved equation (9) and have determined the likelihood  $L$ . We could find the parameters  $(r_0, \dots, c)$  corresponding to the maximum value  $L(r_0, \dots, c)$ .

The results for different  $r_{\max}$  are given in Table 1. As is seen, the distance to the GC is about 8.2–8.4 kpc, lower than that of

the IAU recommended value of  $r_0 = 8.5$  kpc. Summarizing, space distribution modelling of RRLs yields mean  $r_0 = 8.28 \pm 0.14$  kpc,  $\alpha = -2.31 \pm 0.05$ ,  $\theta = -6.5^\circ \pm 0.6^\circ$ ,  $a = 1$ ,  $b = 0.7 \pm 0.04$ , and  $c = 0.7 \pm 0.03$  for the values of the effective bulge radius  $r_{\text{bulge}} = r_{\max} = 2.0, 2.5$ , and  $3.0$  kpc. Our newly deduced value of  $r_0 \approx 8.3$  kpc is  $\approx 0.3$  and  $\approx 0.1$  kpc moderately higher than the estimates derived from the Do et al. (2019) and GRAVITY Collaboration (2019) direct measurements, respectively. The result is consistent (within the uncertainty) with determination of  $r_0$  by direct modelling the space motions of masers (Reid et al. 2019). This value of the solar distance  $r_0$  agrees with our previous estimate  $r_0 = 8.1 \pm 0.2$  kpc from halo RRLs (Griv et al. 2019). It is also fairly consistent with the latest estimations of  $r_0$  by Boehle et al. (2016), de Grijs & Bono (2016), Fritz et al. (2016), Bhardwaj et al. (2017), McMillan (2017), Camarillo et al. (2018), Contreras Ramos et al. (2018), Majaess et al. (2018), and Qin et al. (2018) (see however Catchpole et al. 2016; Saha et al. 2019). Although the distance  $r_0$  we have obtained is similar to the one estimated in our previous paper, it is good to see the same conclusion with new, more accurate and extensive observations. Especially notice that the  $(r_0, \dots, c)$  values for fits with different  $r_{\max}$  in the range 2–4 kpc are almost equal. The latter was already anticipated because the stars are mainly located within  $\approx 3$  kpc from the GC (Fig. 1, right-hand panel).

Interestingly, the power-law index derived from the distribution of halo RRLs is about the same,  $\alpha \approx -2.2$  (Griv et al. 2019). Our working hypothesis is therefore that the old, spherical-like, pressure-supported bulge and halo form an undivided, continuous subsystem in the Galaxy (cf. Alcock et al. 1998, p. 492, ‘the bulk of the RR Lyrae stars represents the inner extension of an axisymmetric halo, while the more metal-rich stars belong to a barred bulge’). The hypothesis is consistent with an old bulge component originating from an early, fast mass assembly, as suggested by many computer simulations (e.g. Pérez-Villegas et al. 2017; Rojas-Arriagada et al. 2017).

The distribution of RRLs has the shape of an ellipsoid slightly elongated almost towards us with a major axis of its symmetry and two minor axes of almost the same length. The elongation along the line of sight is probably an observational bias due to our incomplete longitudinal coverage (Dékány et al. 2013, p. 4). The obtained average ratio of the major axis to the minor axis in the plane and to the vertical axis of the ellipsoid for the values of the effective bulge radius in the range  $r_{\text{bulge}} = 2 - 3$  kpc is  $\approx 1: 0.7: 0.7$ . By a way of contrast, Pietrukowicz et al. (2015) have obtained a ratio of  $\approx 1: 0.5: 0.4$  by using stars from the OGLE sample located only within the central  $\approx 1$  kpc.

In conjunction with the last result, examining Table 1 it is worthnoting that the distribution of stars becomes considerably more spheroidal as  $r_{\max}$  decreases and space distribution of stars with ages  $\gtrsim 10$  Gyr within  $\approx 2$  kpc from the GC is almost spherically symmetric. The latter was also anticipated as most likely due to the

presence of a more axisymmetric concentration of stars in the  $\lesssim 2$  kpc bulge (Dékány et al. 2013; Catchpole et al. 2016; Grady et al. 2020). We conclude that these high  $|b|$  RRLs do not trace a strong bar-like structure in the direction of the Galactic bulge, as  $b/a \sim 1$  and the angle  $|\theta|$  is small. To repeat ourselves, such a model of the bulge is in good accord with Dékány et al.’s (2013) conclusion that unlike young and intermediate-age stars (and gas), age-old stars do not trace a strong bar, but have a more spheroidal distribution (see also Wesselink 1987; Minniti et al. 2017; Prudil et al. 2019). Following Alcock et al. (1998), we argue that the latter is mainly because the dynamical response of old stellar population to the imposed gravitational potential of a bar is expected to be quite different from the response of younger, on the average, population. The difference is likely regulated by a factor which takes into account the fact that the non-axisymmetric potential field of the bar affects only weakly the objects of older population with high random (turbulent) velocities.<sup>4</sup>

Using the following Faber–Jackson relation for black holes, the relation between black hole mass ( $M_{\text{BH}}$ ) and galaxy bulge velocity dispersion ( $\sigma$ ) by McConnell et al. (2011):

$$\frac{M_{\text{BH}}}{10^8 M_{\odot}} \approx 1.9 \left( \frac{\sigma}{200 \text{ km s}^{-1}} \right)^{5.1},$$

one calculates the velocity dispersion of the old stellar population of the Galactic bulge  $\sigma \sim 100 \text{ km s}^{-1}$  (cf. Kunder et al. 2016, figs 2 and 3 therein). As for us, only young and intermediate-age objects with a relatively small velocity dispersion, say,  $\sigma < 70 \text{ km s}^{-1}$ , should show some prominent effects of the bar. Grady et al. (2020) have already suggested that their old Miras (and RRLs of Dékány et al. 2013) are kinematically hot enough not to be caught by the bar potential.

We found that the tilt angle  $\theta \approx -6.5^\circ$ , thus the angle  $|\theta|$  is small. This is inconsistent with Pietrukowicz et al.’s (2015) main result who have demonstrated that spatial distribution of OGLE RRLs has the shape of a triaxial ellipsoid with a major axis located in the Galactic plane and inclined at an angle of  $\theta = 20^\circ \pm 3^\circ$  to the Sun–GC line of sight (see Rattenbury et al. 2007 and Nataf et al. 2013 for earlier OGLE results). The latter is one of cardinal differences between our and the Pietrukowicz et al. (2015) models.

How can we explain the fact that according to Pietrukowicz et al. (2015)  $\theta \approx 20^\circ$  (and even  $\approx 30^\circ$  in the innermost parts of the bulge) and here we found that  $|\theta|$  is small? As mentioned above (Section 1.2), Pietrukowicz et al. (2015) used about 4700 stars from the full OGLE sample in a much smaller area in the inner Galactic bulge with  $-4^\circ < l < +4^\circ$  and  $-6.7^\circ < b < -2.7^\circ$  to derive the parameters of the distribution for the RRLs population. In other words, they studied the 3D structure of the bulge for regions of  $r \lesssim 1$  kpc and as close as  $\approx 0.2$  kpc from the GC (Pietrukowicz et al. 2015, figs 7 and 8 therein).<sup>5</sup> Unlike Pietrukowicz et al. (2015), our method can be applied only to bulge’s objects located at Galactocentric distances  $r > 1$  kpc by adopting a power-law distribution with  $\alpha < 0$  (Fig. 1). It is naturally to expect that these relatively distant regions of the old bulge do not incline to the Sun–GC line of sight. That may explain the apparent contradiction

<sup>4</sup>Observations convincingly indicate an increase in the total velocity spread in the older stars, which is likely due to dynamical relaxation. Searches for both collisional and collisionless relaxation mechanisms have been going on concurrently (e.g. Grivnev & Fridman 1990; Griv, Gedalin & Eichler 2009).

<sup>5</sup>Interestingly, closer to the GC they obtained different values of the tilt angle. In particular, in the innermost region  $\theta$  increases up to about  $30^\circ$ .

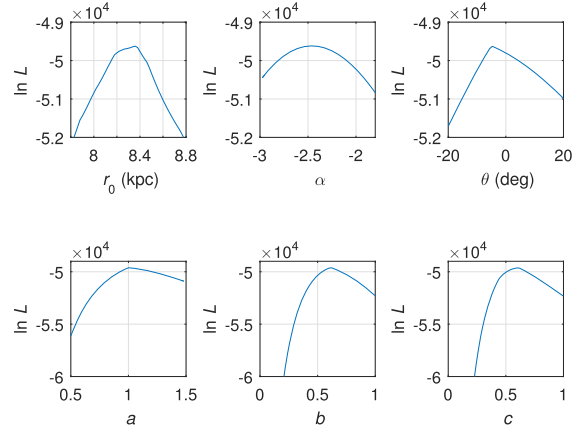


**Figure 4.** For selected 15 334 RRLs of the OGLE sample within the Galactocentric distance  $r_{\text{max}} = 3$  kpc, the natural logarithm of the likelihood  $L$  is plotted against each of six parameters  $r_0$ ,  $\alpha$ ,  $\theta$ ,  $a$ ,  $b$ , and  $c$ ; the other parameters are held fixed in each case.

between our results and those obtained earlier by Pietrukowicz et al. (2015).

One understands after all that our outcome – OGLE RRLs do not trace a strong bar-shaped structure within  $\approx 3$  kpc from the GC, as  $b/a \sim 1$  and  $|\theta| \sim 0^\circ$  – must be regarded as tentative until more extensive data are available. Also, there are additional uncertainties for the  $(r_0, \dots, c)$  fits given in Table 1 above, namely, systematic errors, which are tied in part to uncertainties in the extinction law, the quality of estimation of the absolute brightness derived from the luminosity–metallicity dependence, the period–magnitude relation employed which relies on the distance to the Large Magellanic Cloud adopted and its uncertainty, etc. The dominant uncertainties in the solar distance value are systematic (Gillessen et al. 2009). Pietrukowicz et al. (2015), de Grijs & Bono (2016), and Majaess et al. (2018) have shown that the uncertainty of  $r_0$  is mainly dominated by systematic error, whereas the large number of stars naturally lowers the statistical error. A detailed analysis of the possible causes of systematic errors is out of the scope of this paper; here, we simply use relevant Pietrukowicz et al.’s (2015), de Grijs & Bono’s (2016), and Majaess et al.’s (2018) studies as reference. They have already inferred the systematic errors of about  $\pm 0.4$  kpc. That said, higher quality observations will be necessary to draw firmer conclusions about the solar distance and its uncertainties (see also Hajdu et al. 2020 for a discussion of the problem).

In Fig. 4, the natural logarithm of the likelihood  $L$  is plotted against each parameter for selected RRLs of the OGLE sample within the distance  $r_{\text{max}} = 3$  kpc from the GC. Maxima of  $L$  with respect to  $(r_0, \dots, c)$  are clearly apparent from the simulation.

## 5 SUMMARY

The high latitude 16 221 RRLs of the latest OGLE sample are located towards the old Galactic bulge. The sky distribution of these stars within  $r \leq 4$  kpc (for  $r_0 = 8.1$  kpc) from the GC along with their possible spacial biases (Hajdu et al. 2020) is approximated by the standard power law. The modified Rastorguev et al. (1994) statistical method is again explored to derive required parameters to solve the problem under consideration from the distribution of objects. As a result, the solar distance  $r_0$ , the power-law index  $\alpha$ , and the major axis  $a$  and two minor axes  $b$  and  $c$  of the observed ellipsoid of stars are found. The novelty is that, unlike Griv et al. (2019), we assume

here from the very beginning that the distribution of stars is not spherically symmetric,  $a \neq b \neq c$ , and additionally the tilt angle is  $\theta \neq 0^\circ$ .

Our main results and conclusions are summarized as follows.

(1) The model of space distribution yields the mean solar distance  $r_0 = 8.28 \pm 0.14$  kpc and the exponent in the power law  $\alpha = -2.31 \pm 0.05$  within the effective bulge radius  $r_{\text{bulge}} = 2\text{--}3$  kpc. Our newly derived solar distance is not too far from the Do et al. (2019) and GRAVITY Collaboration (2019) most accurate and recent determinations of  $r_0 \approx 7.95 \pm 0.06$  kpc and  $r_0 \approx 8.18 \pm 0.03$  kpc. Modelling the space motions of masers has also yield about the same (within the uncertainty) value of  $r_0 = 8.15 \pm 0.15$  kpc (Reid et al. 2019). It is also comparable with our previous evaluation  $r_0 = 8.1 \pm 0.2$  kpc from halo RRLs, with the statistical determination  $r_0 = 8.3 \pm 0.2$  kpc (de Grijs & Bono 2016), and with the most respectable estimate from recent literature values  $r_0 = 8.0 \pm 0.3$  kpc (Camarillo et al. 2018).

(2) The power-law indexes derived from the distribution of bulge and halo RRLs are almost the same, namely  $|\alpha| = 2.2\text{--}2.4$ . In the spirit of Alcock et al. (1998), we suggest therefore that the old, spherical-like, pressure-supported bulge and halo form an undivided, continuous subsystem in the Galaxy. The ancient stellar population of the bulge may represent the inner extension of an almost axisymmetric halo.

(3) The space distribution of RRLs has the shape of a triaxial ellipsoid slightly elongated almost towards the Sun with a major axis of its symmetry and two minor axes of almost the same length. The obtained average scale length ratio of the major axis to the minor axis in the plane and to the vertical axis of the ellipsoid within  $r_{\text{bulge}} = 2\text{--}3$  kpc is  $\approx 1: 0.7: 0.7$ . The distribution of RRLs becomes considerably more spheroidal as  $r_{\text{bulge}}$  decreases, that is, both  $b$  and  $c \rightarrow 1$  and sky distribution of stars within  $\approx 2$  kpc from the GC is almost spherically symmetric. Thus, unlike planar gas, young and intermediate-age metal-rich stars, these metal-poor and kinematically hot stars do not trace a strong bar-like structure in the direction of the bulge at distances  $> 1$  kpc from the GC. Alcock et al. (1998) and Dékány et al. (2013) were the first who have made clearly this point.

(4) More data are needed in order to determine whether the old stellar population in the inner regions closer to the GC, say, at distances  $r \lesssim 1$  kpc shows a barred distribution, where the non-axisymmetric bar potential is seemingly strong enough to influence the kinematically hot stellar component. The present sample of OGLE RRLs does not contain a sufficient number of stars to trace the bar-shaped geometry of the inner bulge by using the statistical method.

(5) The tilt angle  $|\theta|$  is small,  $\theta \approx -6.5^\circ$ . The latter is inconsistent with Pietrukowicz et al.'s (2015) result ( $\theta \approx 20^\circ$ ). This is very likely because our method can be applied only to bulge's stars located at distances  $> 1$  kpc from the GC, whereas Pietrukowicz et al.'s sample of stars in the area was specifically done at smaller distances within the central  $\sim 1$  kpc. Further investigations are evidently necessary in order to clarify the issue.

(6) The above results are insensitive to statistical distance errors of stars of the order of  $\pm 5$  per cent. The dominant uncertainties in the solar distance, power-law index, etc., values are systematic ones.

As we have seen above, the impact of the bar's potential would expectedly be seen at smaller  $r$ . The most comprehensive analysis for old bulge RRLs towards lower  $|b|$  (towards smaller  $r$ , correspondingly) along the southern Galactic disc was done by Dékány et al. (2018). Dékány & Grebel (2020) have identified 4314 type-

RRab RRLs in the near-infrared VVV data concentrated to  $|b| \lesssim 1^\circ$ , where most of these stars are beyond the detection limit of optical surveys. Dékány et al. (2019) have discovered over 500 type II Cepheids, located in the inner bulge within  $\sim 1$  kpc from the GC. Similar to bulge RRLs, type II Cepheids, i.e. old ( $\sim 10$  Gyr), typically metal-poor, low-mass ( $\sim 0.5 M_\odot$ ) stars, show a centrally symmetric spatial distribution and high concentration around the GC. A good opportunity to revise the problem is accordingly opened now by these new samples of age-old variable stars.

In closing our discussion of the parameters  $(r_0, \dots, c)$ , we wish to emphasize that they are all independent quantities, so the agreement of the value  $r_0$  we have obtained here with the result obtained from our previous study of the SEKBO RRLs appears quite promising. In the following publication of the series, the conclusions of the work will be discussed, and additional arguments for the solar distance in the range  $r_0 = 8.1\text{--}8.3$  kpc, the power index  $|\alpha| = 2.2\text{--}2.4$ , and the bulge flattening  $q = 0.7\text{--}0.9$  within  $\approx 3$  kpc from the GC will be offered. We are also working on adding more stars to such an analysis, with the goal of reducing measurement uncertainties (in particular, systematic errors) of  $(r_0, \dots, c)$  (e.g. Minniti 2018). Further details will appear elsewhere.

## ACKNOWLEDGEMENTS

We would like to express our gratitude to our colleagues from the Department of Physics, at the Ben-Gurion University and the Department of Physics and Institute of Astronomy, at the National Tsing-Hua University who have discussed with us many of the problems considered in the paper. We are grateful to Irena Zlatopolsky for valuable technical assistance. The authors thank the anonymous referee for the helpful comments, numerous suggestions, and sharp criticisms of some preliminary results that helped us to improve the quality of this paper. The study described here was partially carried out at the NTHU in 2019 November. EG thanks Ing-Guey Jiang for the hospitality he and his colleagues extended to him during a three-weeks long visit in Hsin-Chu. EG is also thankful to the Israeli Ministry of Immigrant Absorption for partial financial support in the framework of the program 'KAMEA'. This study was supported in part by the Israel Science Foundation, the United States-Israel Binational Science Foundation, and the Ministry of Science and Technology of Taiwan.

## DATA AVAILABILITY

The data underlying this article were obtained from the main OGLE Homepage, the University of Warsaw and can be requested through <http://ogle.astro.uw.edu.pl/~ogle/OCVS/>. The derived data generated and analysed in this research will be also shared on request to the corresponding author.

## REFERENCES

- Aguerri J. A. L., Méndez-Abreu J., Corsini E. M., 2009, *A&A*, 495, 491
- Alcock C. et al., 1998, *ApJ*, 492, 190
- Anders F. et al., 2019, *A&A*, 628, A94
- Antoja T. et al., 2014, *A&A*, 563, A60
- Babusiaux C., Gilmore G., 2005, *MNRAS*, 358, 1309
- Bennett M., Bovy J., 2019, *MNRAS*, 482, 1417
- Bhardwaj A. et al., 2017, *A&A*, 605, A100
- Binney J. J., Gerhard O. E., Spergel D., 1996, *MNRAS*, 288, 365
- Bland-Hawthorn J., Gerhard O., 2016, *ARA&A*, 54, 529
- Bobylev V. V., Mosenkov A. V., Bajkova A. T., Gontcharov G. A., 2014, *Astron. Lett.*, 40, 86

- Boehle A. et al., 2016, *ApJ*, 830, 17
- Bonatto C., Bica E., Barbuy B., Ortolani S., 2009, in Richtler T., Larsen S., eds, *Globular Clusters – Guides to Galaxies*, Springer, Berlin, p. 209
- Bovy J., Leung H. W., Hunt J. A. S., Mackereth J. T., García-Hernández D. A., Roman-Lopes A., 2019, *MNRAS*, 490, 4740
- Buta R. J. et al., 2015, *ApJS*, 217, 32
- Camarillo T., Mathur V., Mitchell T., Ratra B., 2018, *PASP*, 130, 24101
- Catchpole R. M., Whitelock P. A., Feast M. W., Hughes S. M. G., Irwin M., Alard C., 2016, *MNRAS*, 455, 2216
- Clarke J. P., Wegg C., Gerhard O., Smith L. C., Lucas P. W., Wylie S. M., 2019, *MNRAS*, 489, 3519
- Contreras Ramos R. et al., 2018, *ApJ*, 863, 79
- de Grijp R., Bono G., 2016, *ApJS*, 227, 5
- Dékány I., Grebel E. K., 2020, *ApJ*, 898, 46
- Dékány I., Minniti D., Catelan M., Zoccali M., Saito R. K., Hempel M., Gonzalez O. A., 2013, *ApJ*, 776, L19
- Dékány I., Hajdu G., Grebel E. K., Catelan M., Elorrieta F., Eyheramendy S., Majaess D., Jordán A., 2018, *ApJ*, 857, 54
- Dékány I., Hajdu G., Grebel E. K., Catelan M., 2019, *ApJ*, 883, 58
- Do T. et al., 2019, *Science*, 365, 664
- Drake A. J. et al., 2013, *ApJ*, 763, 32
- Elmegreen B. G., Elmegreen D. M., 1989, *ApJ*, 342, 677
- Ferguson D., Gardner S., Yanny B., 2017, *ApJ*, 843, 141
- Freeman K. C., Norris J., 1981, *ARA&A*, 19, 319
- Fritz T. K. et al., 2016, *ApJ*, 821, 44
- Genzel R., Eisenhauer F., Gillessen S., 2010, *Rev. Mod. Phys.*, 82, 3121
- Gillessen S., Eisenhauer F., Trippe S., Alexander T., Genzel R., Martins F., Ott T., 2009, *ApJ*, 692, 1075
- Gonzalez O. A., Rejkuba M., Zoccali M., Valenti E., Minniti D., Schultheis M., Tobar R., Chen B., 2012, *A&A*, 543, 13
- Grady J., Belokurov V., Evang N. W., 2020, *MNRAS*, 492, 3128
- GRAVITY Collaboration, 2019, *A&A*, 625, L10
- Griv E., Gedalin M., Eichler D., 2009, *AJ*, 137, 3520
- Griv E., Lin C.-C., Ngeow C.-C., Jiang I.-G., 2014, *New Astron.*, 29, 9
- Griv E., Gedalin M., Jiang I.-G., 2019, *MNRAS*, 484, 218
- Griv E., Gedalin M., Shih I.-C., Hou L.-G., Jiang I.-G., 2020, *MNRAS*, 493, 2111
- Grivnev E. M., Fridman A. M., 1990, *SvA*, 34, 10
- Hajdu G., Dékány I., Catelan M., Grebel E. K., 2020, *Exp. Astron.*, 49, 217
- Harris W. E., 1976, *AJ*, 81, 1095
- Harris W. E., 1996, *AJ*, 112, 487
- Hinkel A., Gardner S., Yanny B., 2020, *ApJ*, 899, L14
- Keller S. C., Murphy S., Prior S., DaCosta G., Schmidt B., 2008, *ApJ*, 678, 851
- Kerr F. J., Lynden-Bell D., 1986, *MNRAS*, 221, 1023
- Khoperskov S., Gerhard O., Di Matteo P., Haywood M., Katz D., Khrapov S., Khoperskov A., Arnaboldi M., 2020, *A&A*, 634, L8
- Kunder A., Chaboyer B., 2008, *ApJ*, 136, 2441
- Kunder A. et al., 2016, *ApJ*, 821, L25
- López-Corredoira M., Garzón F., Hammersley P., Mahoney T., Calbet X., 1997, *MNRAS*, 292, L15
- Majaess D. J., 2010, *Acta Astron.*, 60, 55
- Majaess D. J., Turner D. G., Lane D. J., 2009, *MNRAS*, 398, 263
- Majaess D. J., Dékány I., Hajdu G., Minniti D., Turner D., Gieren W., 2018, *Ap&SS*, 363, 127
- Mateu C., Vivas A. K., 2018, *MNRAS*, 479, 211
- McConnell N. J., Ma C.-P., Gebhardt K., Wright S. A., Murphy J. D., Lauer T. R., Graham J. R., Richstone D. O., 2011, *Nature*, 480, 215
- McMillan P. J., 2017, *MNRAS*, 465, 76
- Miceli A. et al., 2008, *ApJ*, 678, 865
- Minniti D., 2018, in Gionti G., Kikwaya J.-B., Eltu S.J., eds, *Astrophysics and Space Science Proceedings*, Vol. 51, The Vatican Observatory, Castel Gandolfo: 80th Anniversary Celebration, Springer, Berlin, p. 63
- Minniti D. et al., 2010, *New Astron.*, 15, 433
- Minniti D. et al., 2017, *AJ*, 153, 179
- Nataf D. M. et al., 2013, *ApJ*, 769, 88
- Pavlovskaya E. D., Suchkov A. A., 1980, *SvA*, 24, 164
- Pérez-Villegas A., Portail M., Wegg C., Gerhard O., 2017, *ApJ*, 840, L2
- Pettitt A. R., Ragan S. E., Smith M. C., 2020, *MNRAS*, 491, 2162
- Pietrukowicz P., 2020, in Valluri M., Sellwood J. A., eds, *Proc. IAU Symp. 353, Galactic Dynamics in the Era of Large Surveys*. Kluwer, Dordrecht, p. 1
- Pietrukowicz P. et al., 2012, *ApJ*, 750, 169
- Pietrukowicz P. et al., 2015, *ApJ*, 811, 113
- Portail M., Gerhard O., Wegg C., Ness M., 2017, *MNRAS*, 465, 1621
- Prudil Z., Dékány I., Catelan M., Smolec R., Grebel E. K., Skarka M., 2019, *MNRAS*, 484, 4833
- Qin W., Nataf D. M., Zakamska N., Wood P. R., Casagrande L., 2018, *ApJ*, 865, 47
- Queiroz A. B. A. et al., 2020, *A&A*, 638, 76
- Rastorguev A. S., Pavlovskaya E. D., Durlevich O. V., Filipova A. A., 1994, *Astron. Lett.*, 20, 591
- Rattenbury N. J., Mao S., Sumi T., Smith M. C., 2007, *MNRAS*, 378, 1064
- Reid M. J., 1993, *ARA&A*, 31, 345
- Reid M. J. et al., 2019, *ApJ*, 885, 131
- Rojas-Arriagada A. et al., 2017, *A&A*, 601, A140
- Saha A. et al., 2019, *ApJ*, 874, 30
- Saito R. K. et al., 2012, *A&A*, 537, A107
- Sanders J. L., Smith L., Evans N. W., 2019, *MNRAS*, 488, 4552
- Sesar B., Jurić M., Ivezić Z., 2011, *ApJ*, 731, 4
- Sesar B. et al., 2013, *AJ*, 146, 21
- Sesar B. et al., 2017, *AJ*, 153, 204
- Simion I. T., Belokurov V., Irwin M., Koposov S. E., Gonzalez-Fernandez C., Robin A. C., Shen J., Li Z.-Y., 2017, *MNRAS*, 471, 4323
- Skowron D. M. et al., 2019, *Science*, 365, 478
- Sormani M. C., Binney J., Magorrian J., 2015, *MNRAS*, 454, 1818
- Soszyński I. et al., 2014, *Acta Astron.*, 64, 177
- Soszyński I. et al., 2019, *Acta Astron.*, 69, 321
- Surot F. et al., 2019, *A&A*, 629, A1
- Udalski A., Szymański M. K., Szymański G., 2015, *Acta Astron.*, 65, 1
- Valenti E. et al., 2016, *A&A*, 587, L6
- Wegg C., Gerhard O., Portail M., 2015, *MNRAS*, 450, 4050
- Weiland J. L. et al., 1994, *ApJ*, 425, L81
- Wesselink T. J. H., 1987, PhD thesis, Katholieke Univ. Nijmegen
- Zinn R., 1985, *ApJ*, 293, 424